Coulomb blockade conductance-peak distribution of quantum dots under generic conditions: A system-dependent random-matrix approach

Dayasindhu Dey and Pragya Shukla
Department of Physics, Indian Institute of Technology, Kharagpur, India
(Received 23 June 2011; published 23 November 2011)

We present an analytical formulation for the width and the conductance-peak distributions in the Coulomb blockade regime of quantum dots with multichannel leads. The dot's Hamiltonian is modeled by a generalized, Gaussian, multiparametric random-matrix ensemble and is applicable to dots with arbitrary shape or disorder strength, strong or weak two-body interactions, and a generic electron dynamics (chaotic/nonchaotic) inside dot. Our results show that the conductance fluctuations for a wide range of dots can be described by a complexity parameter-based common mathematical formulation.

DOI: 10.1103/PhysRevB.84.195318 PACS number(s): 73.63.Kv, 42.50.Lc, 73.23.−b

I. INTRODUCTION

Coulomb blockade conductance fluctuations, an important characteristic of the transport phenomena in almost closed quantum dots, have motivated intense research efforts during the past two decades.[1] Most of these studies, however, have focused on the dots with chaotic, single-particle dynamics. The scientific quest as well as industrial significance makes it relevant to seek the information for dots with more generic features (e.g., those of arbitrary shapes) with or without disorder and electron-electron (e-e) interactions. It is also desirable, if possible, to formulate the conductance fluctuations in a mathematical form applicable to a wide range of almost closed dots. We derive here the formulation in the quantum Coulomb blockade (QCB) regime where temperature ranges are comparable to or smaller than the mean level spacing of the resonances. The generic conditions of the dot-lead system are taken into account by a system-dependent random-matrix model of the dot Hamiltonian.

The conductance fluctuations in almost closed dots originate from the spatial fluctuations of individual resonance wave functions (i.e., the eigenfunctions of dot Hamiltonian) at dot-lead interfaces.[1] As is well known, the eigenfunction fluctuations are sensitive to the nature of the electron dynamics. Based on the dot shape, the dynamics (even in absence of disorder) can be chaotic, integrable, or nonintegrable and the randomness may arise due to scattering from the boundaries. For chaotic shape and/or weak disorder, the quantum dynamics, in a physically relevant basis, is delocalized and almost all matrix elements of the dot Hamiltonian are *effectively* of the same order. The dot Hamiltonian can then be well modeled by the Wigner-Dyson random-matrix ensembles (WDE) which consist of Hermitian matrices with independent, Gaussian distributed elements, of zero mean and the same variance for almost all of them[2] (also referred to as classical or stationary or standard random-matrix ensembles). The observed universal statistical fluctuations[1] of the energy levels and eigenfunctions of the dot Hamiltonian can also be explained by the basis-invariant nature of these ensembles.

Many dot properties (e.g., conductance) can be formulated in terms of the eigenfunctions and eigenvalues of the dot Hamiltonian. This suggests the Wigner-Dyson ensembles as good models for the conductance fluctuations of chaotic/weakly disordered dots.[3] At low temperatures and in the Coulomb blockade regime, however, the experimentally observed fluctuations show deviation from the Wigner-Dyson models; the deviation seems linked to dominance of the nonhomogeneous particle interactions at low temperatures.[4–6] The efforts to include the interactions led to various mathematical models, for example, the constant interaction model,[7] uniform Hamiltonian (also known as the constant interaction and exchange model),[8–10] the constant interaction plus spin-degenerate random-matrix model, the constant interaction plus spin-resolved random-matrix model, the random-interaction matrix model (RIMM),[11] etc. The interaction in almost all these models (except RIMM) is taken into account by adding a constant interaction background to Wigner-Dyson ensembles; the models therefore fail to mimic the generic nature of e-e interactions inside the dot. RIMM attempts to improve this drawback by modeling the complicated particle interactions by a random matrix; RIMM Hamiltonian is $H = V + U$ with V and U representing one- and two-body interactions, both chosen from Wigner-Dyson ensembles. The choice restricts the applicability of RIMM to chaotic or weakly disordered dots with homogenized electron-electron interactions. To model the cases with mixed or diffusive dynamics and/or nonhomogeneous interactions inside the dot, a generalization of RIMM is desirable.

In general, the single-particle dynamics inside an arbitrary shaped ballistic dot is classically nonintegrable and corresponding wave function intensity is nonhomogeneous in position as well as momentum basis (due to inhomogeneous scattering from the dot boundaries). The matrix elements of V can therefore be of varying strengths. A similar form of V results for a disordered dot (inhomogeneous impurity scattering leading to partially localized electron waves). The theoretical treatment of the Hamiltonian in this regime therefore requires a more generalized (i.e., system-dependent) random-matrix approach. (Note, in this case, the Wigner-Dyson model is not applicable even in the absence of the e-e interactions). The dynamics is further complicated by the presence of local particle interactions. In general, the presence of correlated disorder and/or e-e interactions may lead to nonzero correlations among elements of the Hamiltonian. This motivates us to consider an ensemble of H matrices with a multiparametric Gaussian ensemble density with independent or correlated matrix elements.

Our objective in this paper is to formulate the statistics of the Coulomb blockade peak heights in terms of that of the eigenfunctions. The required connection formula, of the conductance-peak heights with eigenfunctions of the dot Hamiltonian, is reviewed in Sec. II. A prior knowledge of the eigenfunction statistics is also needed. This depends on the choice of the ensemble for the dot Hamiltonian; Sec. III introduces our choice (i.e., the generalized Gaussian ensemble) where system dependence enters through the distribution parameters.[12] As shown in Ref. 13, the eigenfunction statistics of this multiparametric ensemble is governed by a single parameter, referred to as the complexity parameter. This information along with the relations given in Secs. II and III is used in Sec. IV to derive the diffusion equations for distributions of the partial width amplitudes and the partial widths, respectively, and subsequently for the peak heights. Section V discusses the solution of the diffusion equation for the peak heights. We conclude in Sec. VI with a summary of our results and open problems.

II. CONDUCTANCE-PEAK HEIGHTS AND RESONANCE EIGENFUNCTIONS

This section reviews the necessary formulas for the QCB conductance in a two-lead dot (see Ref. 1 for details), required later for our analysis.

An almost closed or "isolated" quantum dot can be described as an island of electrons weakly coupled to two leads via tunnel junctions. Under these conditions, a typical resonance width in the dot is smaller than the average spacing Δ between the resonances. As a consequence, only the resonance Ψ with energy E_Ψ closest to the scattering energy E contributes significantly to the zero-temperature conductance: $G(E,T=0)=\frac{e^2}{h}\frac{\Gamma_\Psi^{(l)}\,\Gamma_\Psi^{(r)}}{(E-E_\Psi)^2+(\frac{\overline{\Gamma}_\Psi}{2})^2}$, where

$$\Gamma_\Psi^{(x)}=\sum_c |\gamma_{cx}|^2 \tag{1}$$

is the width of the resonance Ψ to decay into the lead "x" ($x=l,r$ referring to left and right) with γ_{cx} as the partial width amplitude of the resonance level Ψ to decay into channel c of the lead. γ_{cx} can be expressed as a scalar product of the resonance wave function $\Psi=(\psi_1,\psi_2,\ldots,\psi_N)$ and channel wave function $\Phi_c^{(x)}=(\Phi_{1c}^{(x)},\Phi_{2c}^{(x)},\ldots)$:

$$\gamma_{cx}=\left\langle \Phi_c^{(x)}\middle|\Psi\right\rangle \tag{2}$$

(see p. 933 of Ref. 1 for a detailed definition of γ_c).

The finite-temperature conductance $G(E,T)$ is obtained by convoluting $G(E,T=0)$ with a derivative of the Fermi-Dirac distribution (see Sec. D and Eq. (11) of[1]). In the experimentally interesting regime $\overline{\Gamma}\ll T\ll\Delta$ (with $\overline{\Gamma}$ as the average width), the conductance occurs only by the resonant tunneling through the corresponding energy level of the dot and $G(E,T)$ can be approximated as

$$G(E,T)\approx\alpha\; g_\Psi\left[\cosh\left(\frac{E_\Psi-E}{2kT}\right)\right]^{-2}, \tag{3}$$

where $E\approx E_F$ (due to main contribution to conductance from the electrons at Fermi level E_F) and

$$g_\psi=\frac{2}{\overline{\Gamma}_\Psi}\;\frac{\Gamma_\Psi^{(l)}\Gamma_\Psi^{(r)}}{\Gamma_\Psi^{(l)}+\Gamma_\Psi^{(r)}} \tag{4}$$

is the single-level conductance-peak height measured in units of $\alpha=\frac{e^2}{h}\frac{\pi\overline{\Gamma}_\Psi}{4kT}$.

The weak dot-lead coupling leads to Coulomb blockade oscillations of the peak heights as a function of the gate voltage. Detailed information about these oscillations can be obtained from the distribution of peak heights and peak spacings. At finite temperatures, in general, the thermal as well as dynamical correlations among peaks make it necessary to consider the joint distribution of the peak heights of many resonances. At low temperatures $T\leqslant\Delta$, the thermal correlations are exponentially suppressed and only the correlations induced by dynamical modulation dominate. The individual peak-height distribution essentially being a local measure, it is not strongly sensitive to the dynamical correlations (see the results and discussion of Ref. 14). This allows us to consider the peak-height distribution of each resonance separately. As is clear from Eqs. (1) and (2), the distribution $P_g(g_\Psi)$ of g_Ψ can be derived if the statistics of the components $(\psi_1,\psi_2,\ldots,\psi_N)$ of the eigenfunction Ψ is known.

III. ENSEMBLE FOR DOT HAMILTONIAN AND EIGENFUNCTION STATISTICS

The electron dynamics inside an almost closed quantum dot can be described by the dot Hamiltonian $H=V+U$ where

$$\begin{aligned} V&=\sum_{mn} e_{mn}\; a_m^\dagger\; a_n,\\ U&=\sum_{mnrs} u_{mnrs}\; a_m^\dagger\; a_n^\dagger\; a_r\; a_s, \end{aligned} \tag{5}$$

with e_{mn} as the matrix elements of the single-particle Hamiltonian V and u_{mnrs} as the measures of the two-body interaction U. For a clear exposition of our ideas, we now consider the Hamiltonian cases with correlated/uncorrelated elements separately.

A. Hamiltonian with uncorrelated matrix elements

Let us first consider the cases where e-e interaction is negligible, resulting in $H\approx V$. Assuming a white-noise disorder $\langle V(r)V(r')\rangle=\delta(r-r')$, and, choosing a fixed basis of N single-particle states $|m\rangle=a_m^\dagger|0\rangle$, the H matrix can be modeled by an uncorrelated Gaussian ensemble:

$$\rho(H,h,b)=C\exp\left[-\sum_{k,l=1;k\leqslant l}^{N}\frac{1}{2h_{kl}}\,(H_{kl}-b_{kl})^2\right], \tag{6}$$

with h as the variance matrix with $h_{kl}=\langle H_{kl}^2\rangle-\langle H_{kl}\rangle^2=\langle V_{kl}^2\rangle-\langle V_{kl}\rangle^2$ and b as the mean value matrix with $b_{kl}=\langle H_{kl}\rangle=\langle V_{kl}\rangle$.

Based on the complexity of the system, the elements of the parametric matrices h,b can have various functional forms (e.g., exponential, power law, etc). For example, the limit $h_{kl}\to 0$, corresponds to a nonrandom nature of H_{kl}, the limit

$h_{kl} \to \lambda(1+\delta_{kl})/2$, $b_{kl} \to 0$ leads to a Gaussian orthogonal ensemble $\rho(H) = Ce^{-\mathrm{Tr}H^2}$, etc.

In the presence of both disorders, as well as e-e interactions, the electron dynamics is governed by the intercompetition between them. Again assuming a white noise disorder and by choosing now a many-particle basis, H can still be modeled by the ensemble (6). As an example, consider two electrons in an N-sites lattice. It is then appropriate to represent H in a N^2-dimensional basis of the two-particle states $|kl\rangle$; for bookkeeping, we write $|kl\rangle \equiv |\varphi_{(k-1)N+l}\rangle$. With $\mu = (i-1)N + j, \nu = (k-1)N + l$, Eq. (5) then gives

$$H_{\mu\nu} = \langle\varphi_\mu|H|\varphi_\nu\rangle \equiv \langle ij|V|kl\rangle + \langle ij|U|kl\rangle, \tag{7}$$

where

$$\begin{aligned}\langle ij|V|kl\rangle &= V_{ik}\delta_{jl} + V_{il}\delta_{jk} + V_{jk}\delta_{il} + V_{jl}\delta_{ik},\\ \langle ij|U|kl\rangle &= U_{ijkl} + U_{kjil} + U_{ilkj} + U_{klij}.\end{aligned} \tag{8}$$

For cases where both V,U consist of uncorrelated matrix elements, the ensemble H can then be represented by Eq. (6) with indices $\{k,l\}$ replaced by $\{\mu,\nu\}$ (thus $H_{kl} \to H_{\mu\nu}, h_{kl} \to h_{\mu\nu}, b_{kl} \to b_{\mu\nu}$); As is clear from Eq. (7), both the mean and the variance now depend on disorder as well as interaction strength.

The variation of system conditions (e.g., gate voltage, disorder strength, particle density, etc.) results in a variation of the distribution parameters $\{h,b\}$. This leads to an evolution of the H ensemble which, however, is governed by the rescaled complexity parameter Λ [a function of all distribution parameters; see Eqs. (10) and (11) given below].[12] This, in turn, also results in a Λ-governed diffusion of the eigenfunctions of H. As discussed in Ref. 13, the diffusion of the joint probability distribution $P_{N1}(\Psi) \equiv P_{N1}(\psi_1, \ldots, \psi_N)$ of the components ψ_j, $j = 1 \to N$ of a resonance eigenfunction Ψ of H can be given as

$$\frac{\partial P_{N1}}{\partial \Lambda_\Psi} = \sum_{n=1}^{N} \frac{\partial}{\partial \psi_n}\left((N-1)\psi_n + \sum_{m=1}^{N}\frac{\partial}{\partial \psi_m}(\delta_{mn} - \psi_n\ \psi_m)\right) \times P_{N1}, \tag{9}$$

where $\Lambda_\Psi = (\chi/2)\,\Lambda$ with Λ as the rescaled complexity parameter:

$$\Lambda = \frac{Y - Y_0}{\Delta_\xi^2}, \tag{10}$$

with $\Delta_\xi(E)$ as the local mean level spacing of the dot at energy E, χ related to the average localization length ξ of the eigenfunction Ψ, and Y and Y_0 as the complexity parameters for the ensemble and its initial state.[13] Here,

$$Y = -\frac{1}{4N^2\lambda}\ln\left[\prod_{k\leqslant l}{}' |1 - (2-\delta_{kl})h_{kl}/\lambda|\quad |b_{kl}|^2\right] + C_y. \tag{11}$$

Here $\prod'$ implies a product over nonzero b_{kl}, λ is an arbitrary parameter, giving the variance of the matrix elements at the end of the evolution (which can be scaled out without loss of generality), and C_y is an arbitrary constant of integration.

For later reference, it must be mentioned that the steady-state limit $\frac{\partial P_{N1}}{\partial \Lambda_\Psi} = 0$ (or $\Lambda_\Psi \to \infty$) of Eq. (9) corresponds to $h_{kl} \to \lambda(1+\delta_{kl})/2$, $b_{kl} \to 0$. The latter in turn corresponds to the Wigner-Dyson limit of the ensemble (6).

For clarification, we consider two specific models, considered in the past to study interaction effects in quantum dots.

Example (i): Anderson model with Coulomb interaction.[5] This corresponds to V in Eq. (5) as a one-body Anderson Hamiltonian with onsite disorder and nonrandom, isotropic, nearest-neighbor hopping t, and U as the two-body Coulomb interaction between the spinless electron, that is,

$$\begin{aligned} e_{mn} &= \epsilon_m\,\delta_{mn} + t f_{mn},\\ u_{mnrs} &= u_{mn}\,\delta_{mr}\,\delta_{ns} = U_0\left\langle\frac{1}{|r_m - r_n|}\right\rangle,\end{aligned} \tag{12}$$

with $f_{mn} = 1$ for the sites (m,n) as nearest neighbors, $f_{mn} = 0$ otherwise.

The elements $H_{\mu\nu} = V_{\mu\nu} + U_{\mu\nu}$ are now [with $\mu = (i-1)N + j$, $\nu = (k-1)N + l$] as follows:

$$\begin{aligned} V_{\mu\nu} &= \epsilon_i(\delta_{ik}\delta_{jl} + \delta_{il}\delta_{jk}) + \epsilon_j(\delta_{jk}\delta_{il} + \delta_{jl}\delta_{ik})\\ &\quad + t(f_{ik}\delta_{jl} + f_{il}\delta_{jk} + f_{jk}\delta_{il} + f_{jl}\delta_{ik}), \end{aligned} \tag{13}$$

$$U_{\mu\nu} = u_{ij}\ (\delta_{ik}\delta_{jl} + \delta_{il}\delta_{jk})(1 - \delta_{ij}). \tag{14}$$

Assuming onsite energies ϵ_m to be Gaussian distributed with mean zero and variance σ^2, we get

$$\begin{aligned} b_{\mu,\nu} &= t(1+\delta_{ij})f_{xy} && \text{if } x = i \text{ or } j, \text{ and } y = k \text{ or } l,\\ &= 2u_{ij}\ (1-\delta_{ij}) && \text{if } (k = i,\ l = j) \text{ or } (k = j,\ l = i),\\ &= 0 && \text{for other } (\mu,\nu) \text{ pairs.}\end{aligned} \tag{15}$$

Further as U is nonrandom, the contribution to $h_{\mu\nu}$ comes only from V:

$$\begin{aligned} h_{\mu,\nu} &= 2\sigma^2(8\delta_{ij} + (1-\delta_{ij})) && \text{if } \nu = \mu = (i-1)N + j,\\ &= 2\sigma^2(1-\delta_{ij}) && \text{if } \nu = (j-1)N + i,\\ &= 0 && \text{for other } (\mu,\nu) \text{ pairs.}\end{aligned} \tag{16}$$

Substitution of Eqs. (15) and (16) in Eq. (11) gives

$$\begin{aligned} Y = \frac{1}{2N}\ln[|1 - 16\sigma^2|\ |1 - 4\sigma^2|^2(2)^{4z}\ (t)^{4z}\\ \times (2\langle u_{ij}\rangle)^{2(N-1)}] + C_y, \end{aligned} \tag{17}$$

with z as the number of nearest neighbors to each site.

Example (ii): Anderson model with coulomb interaction and on-site spin-interaction.[6] To consider spin effects, this model includes, in addition to the long-range Coulomb interaction among electrons at different sites, an onsite interaction between the electrons of opposite spins.[6] Thus, again we have $H = V + U$ with $U = U_1 + U_2$ where

$$U_1 = -\sum_{m\neq n,s,s'} u_{mn}\ a^\dagger_{ms}\ a_{ms}\ a^\dagger_{ns'}\ a_{ns'}, \tag{18}$$

$$U_2 = \kappa\ \sum_{m,s} a^\dagger_{ms}\ a_{ms}\ a^\dagger_{ms}\ a_{ms}. \tag{19}$$

Note V is similar to the previous case but with electron spin included:

$$V = \sum_{m,s}\epsilon_m\ a^\dagger_{ms}a_{ms} + t\sum_{m,n;s} f_{mn}\ a^\dagger_{ms}\ a_{ns}. \tag{20}$$

Confining to the case of two electrons in an N-sites lattice, the matrix elements of H can again be represented by a two-particle basis $|ks;ls'\rangle$:

$$\begin{aligned}&\langle is_1;js_2|H|ks_1;ls_2\rangle\\&\quad= V_{ik}\,\delta_{jl}+V_{jl}\,\delta_{ik}+\big(2u_{ij}+\kappa\,\delta_{jk}\big(1-\delta_{s_1s_2}\big)\big)\,\delta_{ik}\,\delta_{jl},\end{aligned}\tag{21}$$

$$\begin{aligned}&\langle is_1;js_2|H|ks_2;ls_1\rangle\\&\quad= V_{jk}\,\delta_{il}+V_{il}\,\delta_{jk}+\big(2u_{ij}+\kappa\,\delta_{jl}\big(1-\delta_{s_1s_2}\big)\big)\,\delta_{il}\,\delta_{jk}.\end{aligned}\tag{22}$$

It is easy to check that, except for the above two types, all other matrix elements of H are zero.

For notational ease, we again write

$$\begin{aligned}|is_1;js_2\rangle&\equiv\varphi_\mu,\quad\text{with}\quad\mu=N_s\big((i-1)N+j\big)+I(s_1,s_2),\\|ks_3;ls_4\rangle&\equiv\varphi_\nu,\quad\text{with}\quad\nu=N_s\big((k-1)N+l\big)+I(s_3,s_4),\end{aligned}\tag{23}$$

with N_s as the size of the two-particle spin space ($N_s=4$ for the two-electron case). Here $I(s,s')$ is an integer dependent on (s,s'): $I=0\to N_s-1$ for $(s,s')=(-1/2,-1/2),(-1/2,1/2),(1/2,-1/2),(1/2,1/2)$, respectively. The matrix elements of H can again be written as $H_{\mu\nu}$ with $b_{\mu\nu}$ as the mean and $h_{\mu\nu}$ as the variance. For nonrandom hopping t and Gaussian distributed ϵ_k (with $\langle\epsilon_k\rangle=0$ and variance σ^2), Eq. (22) gives

$$\begin{aligned}b_{\mu\nu}&=t(f_{ik}\delta_{jl}+f_{jl}\delta_{ik})+\big(2u_{ij}+\kappa\delta_{jk}\big(1-\delta_{s_1s_2}\big)\big)\delta_{ik}\delta_{jl}\\&\qquad\text{if}\quad\varphi_\nu\equiv|ks_1;ls_2\rangle,\\&=t(f_{jk}\delta_{il}+f_{il}\delta_{jk})+\big(2u_{ij}+\kappa\delta_{jl}\big(1-\delta_{s_1s_2}\big)\big)\,\delta_{il}\delta_{jk}\\&\qquad\text{if}\quad\varphi_\nu\equiv|ks_2;ls_1\rangle,\\&=0\qquad\text{for other }(\mu,\nu)\text{ pairs.}\end{aligned}\tag{24}$$

Again both U_1 and U_2 being nonrandom, the contribution to $h_{\mu\nu}$ comes only from V:

$$\begin{aligned}h_{\mu,\nu}&=2\sigma^2\,(1+\delta_{kj})\delta_{ik}\delta_{jl}\qquad\text{if }\varphi_\nu\equiv|ks_1;ls_2\rangle,\\&=2\sigma^2\,(1+\delta_{lj})\delta_{il}\delta_{jk}\qquad\text{if }\varphi_\nu\equiv|ks_2;ls_1\rangle,\\&=0\qquad\text{for other }(\mu,\nu)\text{ pairs.}\end{aligned}\tag{25}$$

Substitution of Eqs. (15) and (16) in Eq. (11) gives

$$Y=\frac{4N^2}{N_p}\ln\big[(t)^{4z}\,\alpha^{\frac{1}{N}}\,(2\langle u_{kl}\rangle)\,|1-4\sigma^2|\,|1-2\sigma^2|\big]+C_y,\tag{26}$$

with $N_p=N\big(N_s(N-1)/2+1\big)$.

B. Hamiltonian with pairwise correlated elements

Under generic conditions, the impurity distribution inside the dot may lead to pairwise correlations among V-matrix elements: $\langle V_{kl}V_{ij}\rangle\neq0$. The e-e interaction may also result in pair correlations among U- elements i.e $\langle U_{ijkl}U_{klmn}\rangle\neq0$. H then turns out to be a matrix with a varying degree of correlations among its elements and can be represented by an ensemble density,

$$\rho(H,a,b)=C\exp\left[-\sum_{i,j,k,l}b_{ijkl}H_{ij}H_{kl}-\sum_{k,l}a_{kl}H_{kl}\right],\tag{27}$$

with C as a normalization constant. As discussed in Ref. 13, the evolution of P_{N1} in this case can again be described by Eq. (9) with Λ given by Eq. (10), however, now

$$Y=\sum_{kl}\int da_{kl}\,\frac{v_{kl}}{A_{kl}}+\sum_{klrmn}\int db_{klmn}\,\frac{w_{klmn}}{B_{klmn}}+C_y,\tag{28}$$

where v_{kl} and w_{klmn} are arbitrary constants. Furthermore,

$$\begin{aligned}A_{kl}&=\gamma\;a_{kl}-\sum_{mn}(1+\delta_{mn})\,a_{mn}\;b_{klmn}\;f_{klmn},\\B_{klmn}&=\gamma b_{klmn}-(1/2)\sum_{ij}(1+\delta_{ij})\,b_{klij}\;b_{mnij}\;f_{klij}\;f_{ijmn}.\end{aligned}\tag{29}$$

Here $f_{klkl}=2$ and $f_{klmn}=1$ [for $(kl)\neq(mn)$].

IV. SINGLE-PARAMETRIC DIFFUSION OF CONDUCTANCE DISTRIBUTION

Equation (4) describes the conductance in terms of the partial widths which in turn can be expressed in terms of the partial-width amplitudes. Prior to derivation of the diffusion equation for the conductance distribution, we therefore need to obtain the diffusion equations for the partial-width amplitudes and subsequently the partial widths.

A. Diffusion equation for the partial-width amplitudes

For a dot connected with two leads, the distribution $P_\gamma(\gamma_l,\gamma_r)$ of the partial-width amplitudes $(\gamma_l,\gamma_r)\equiv(\gamma_{1l},\ldots,\gamma_{N_ll},\gamma_{1r},\ldots,\gamma_{N_rr})$ for a resonance ψ is given by

$$P_\gamma(\gamma_l,\gamma_r)=\int\;D\Psi\;f_l\;f_r\;P_{N1}(\Psi),\tag{30}$$

where $D\Psi=\prod_{j=1}^{N}d\psi_j$.

$$f_l=\prod_{c=1}^{N_l}\delta(\gamma_{cl}-X_{cl}),\quad f_r=\prod_{c=1}^{N_r}\delta(\gamma_{cr}-X_{cr}).\tag{31}$$

Here subscripts l,r refer to left and right leads, with N_l and N_r as the total number of channels in them, respectively. Further $X_{cx}=\sum_j\Phi_{cj}^{(x)*}\psi_j=\sum_j\Phi_{cj}^{(x)}\psi_j$ are the partial-width amplitudes to decay into channel c in the lead x ($x=l,r$). Note, due to time-reversal symmetry of the dot-lead Hamiltonian, the components ψ_j and Φ_{cj} can be chosen real.

The effect of the varying system condition on P_γ can now be obtained from Eq. (9),

$$\frac{\partial P_\gamma}{\partial\Lambda_\psi}=I_1+I_2+I_3,\tag{32}$$

where

$$I_1 = (N-1)\int D\Psi\ f_l\ f_r \sum_{n=1}^{N} \frac{\partial}{\partial \psi_n}(\psi_n P_{N1}), \quad (33)$$

$$I_2 = \int D\Psi\ f_l\ f_r \sum_{n=1}^{N} \frac{\partial^2 P_{N1}}{\partial \psi_n^2}, \quad (34)$$

$$I_3 = \int D\Psi\ f_l\ f_r \sum_{m,n=1}^{N} \frac{\partial^2}{\partial \psi_n \partial \psi_m}(\psi_n \psi_m P_{N1}). \quad (35)$$

The next step is to rewrite the integrals in Eqs. (33)–(35) in terms of the γ derivatives. Using partial integration and the relations,

$$\frac{\partial(f_l\ f_r)}{\partial \psi_k} = -\sum_{x=(l,r)} \sum_{p} \frac{\partial(f_l\ f_r)}{\partial \gamma_{px}} \frac{\partial X_{px}}{\partial \psi_k}, \quad (36)$$

and $\frac{\partial X_{px}}{\partial \psi_k} = \Phi_{kp}^{(x)*}$, I_1 can be reduced as

$$I_1 = (N-1) \sum_{x=(l,r)} \sum_{p} \frac{\partial}{\partial \gamma_{px}}(\gamma_{px} P_\gamma). \quad (37)$$

Here $\sum_p$ refers to the sum over all channels in the lead "x".

Similarly a repeated partial integration and the relation $\frac{\partial^2 X_{px}}{\partial \psi_k^2} = 0$ (for all p,k), simplifies I_2:

$$I_2 = 2 \sum_{p,q} \sum_{x,y=l,r} \frac{\partial^2 \left(M_{pq}^{(xy)} P_\gamma\right)}{\partial \gamma_{px} \partial \gamma_{qy}}. \quad (38)$$

Here $M_{pq}^{(xy)}$ is the correlation between the q^{th} and p^{th} channels of the leads "x" and "y," respectively:

$$M_{pq}^{(xy)} = \sum_n \phi_{np}^{(x)} \phi_{nq}^{(y)} = \left\langle \Phi_p^{(x)} \middle| \Phi_q^{(y)} \right\rangle. \quad (39)$$

Furthermore, I_3 can be expressed as a second-order derivative,

$$I_3 = -\sum_{x,y=l,r} \sum_{p,q} \frac{\partial^2(\gamma_{px}\gamma_{qy} P_\gamma)}{\partial \gamma_{px} \partial \gamma_{qy}}. \quad (40)$$

Substitutions of Eqs. (37), (38), and (40) in Eq. (32) gives the Λ_ψ-governed diffusion equation of the partial-width amplitudes:

$$\frac{\partial P_\gamma}{\partial \Lambda_\psi} = \sum_{x=l,r} \sum_{p} \frac{\partial}{\partial \gamma_{px}} \left(\gamma_{px} P_\gamma + \sum_{y=l,r} \sum_{q} \frac{\partial}{\partial \gamma_{qy}} \times \left(M_{pq}^{(xy)} + \gamma_{px}\gamma_{qy} \right) P_\gamma \right). \quad (41)$$

Equation (41) describes the Λ-governed diffusion of the joint probability distribution of N_l and N_r partial widths in the left and right lead, respectively. This can now be used to derive the joint distribution of the left and right resonance widths.

B. Diffusion equation for the resonance widths

Following Eq. (1), the peak width distribution for the resonance ψ can be given as

$$P_\Gamma(\Gamma_l, \Gamma_r) = \int \prod_{x=l,r} \delta\left(\Gamma_x - \sum_i \gamma_{ix}^* \gamma_{ix}\right) P_\gamma(\gamma_l, \gamma_r)\ D\gamma_l D\gamma_r, \quad (42)$$

with $D\gamma_x = \prod_j \gamma_{jx}$. Henceforth the subscript Ψ on Γ_x will be suppressed unless necessary for discussion.

As discussed in Ref. 16, the Wigner-Dyson limit of P_Γ depends on the channel correlation matrix M. For the case of uncorrelated and equivalent channels ($\Gamma_l = \Gamma_r = \Gamma$), M has all degenerate eigenvalues which results in a χ_ν^2 distribution of P_Γ (with $\nu = \beta N_c$ as the degrees of freedom):[11]

$$P_\Gamma(\Gamma) \propto \Gamma^{\nu/2-1} \exp[-\nu\Gamma/2\overline{\Gamma}]. \quad (43)$$

Under generic conditions, however, the channels are correlated (nonorthogonal) and nonequivalent (i.e., different average partial widths). The determination of $P_\Gamma(\Gamma_l, \Gamma_r)$, in general, by the integration route [given by Eq. (42)] is technically complicated even in the Wigner-Dyson limit of P_γ [i.e., Porter-Thomas distribution for P_{N1}; see Eqs. (126) and (127) of Ref. 1]. For the multiparametric Gaussian ensemble case, we therefore proceed by an alternative route, based on the complexity parameter-governed evolution of P_Γ.

Differentiating Eq. (42) with respect to Λ_ψ we get

$$\frac{\partial P_\Gamma}{\partial \Lambda_\psi} = \int \frac{\partial P_\gamma}{\partial \Lambda_\psi}\ \delta_l\ \delta_r\ d\gamma^{(l)} d\gamma^{(r)}, \quad (44)$$

where $\delta_x = \delta(\Gamma_x - \sum_i \gamma_{ix}^* \gamma_{ix})$. Substitution of Eq. (41) in Eq. (44) results in

$$\frac{\partial P_\Gamma}{\partial \Lambda_\psi} = (J_1 + J_2 + J_3), \quad (45)$$

where

$$J_1 = (N-1) \int \delta_l\ \delta_r \sum_{x=l,r} \sum_{p} \left[\frac{\partial}{\partial \gamma_{px}}(\gamma_{px} P_\gamma) \right] D\gamma, \quad (46)$$

$$J_2 = \int \delta_l\ \delta_r \sum_{x,y} \sum_{p,q} \left[\frac{\partial^2}{\partial \gamma_{px} \partial \gamma_{qy}} \left(M_{pq}^{(xy)} P_\gamma \right) \right] D\gamma, \quad (47)$$

$$J_3 = \int \delta_l\ \delta_r \sum_{x,y} \sum_{p,q} \left[\frac{\partial^2}{\partial \gamma_{px} \partial \gamma_{qy}} (\gamma_{px}\gamma_{qy} P_\gamma) \right] D\gamma. \quad (48)$$

Using the relation,

$$\frac{\partial}{\partial \gamma_{px}}(\delta_l\ \delta_r) = -\sum_t \frac{\partial(\delta_l\ \delta_r)}{\partial \Gamma_x} \frac{\partial}{\partial \gamma_{px}}\left(\gamma_{tx}^2\right), \quad (49)$$

and partially integrating, we can reduce J_1, J_2, J_3 as

$$J_1 = 2(N-1) \sum_{x=l,r} \frac{\partial}{\partial \Gamma_x}(\Gamma_x P_\Gamma), \quad (50)$$

$$J_2 = 4 \sum_{x=l,r} \left[\sum_{y=l,r} \frac{\partial^2 F_{xy}}{\partial \Gamma_x \Gamma_y} - 2N_x \alpha_x \frac{\partial P_\Gamma}{\partial \Gamma_x} \right], \quad (51)$$

$$J_3 = -4\sum_{x,y=l,r}\left[\frac{\partial^2}{\partial\Gamma_x\partial\Gamma_y}(\Gamma_x\Gamma_y P_\Gamma)\right] + 2\sum_{x=l,r}\left[\frac{\partial}{\partial\Gamma_x}(\Gamma_x P_\Gamma)\right], \tag{52}$$

where α_x is the average diagonal element of the channel matrix of lead "x":

$$\alpha_x = \overline{\langle\Phi_p^x|\Phi_p^x\rangle} = \frac{1}{N_x}\sum_p M_{pp}^{(xx)} = \frac{1}{N_x}\mathrm{Tr}M^{xx} = \overline{M_{pp}^{xx}}, \tag{53}$$

with "$\overline{a_p}$" implying average of a_p over p, and

$$F_{xy} = F_{yx} = \int \delta_l\ \delta_r\ \chi_{xy}\ P_\gamma\ D\gamma, \tag{54}$$

with $\chi_{xy} = \sum_{p,q} M_{pq}^{(xy)}\gamma_{px}\gamma_{qy}$.

In general, the correlations between different channels on the same lead are expected to be weaker as compared to self-correlations, that is, $M_{pp}^{(xx)} \gg M_{pq}^{(xx)}$. Further approximating each diagonal $M_{pp}^{(xx)}$ by the average diagonal α_x, one can approximate $\chi_{xx} \approx \alpha_x \sum_p \gamma_{px}^2$. On substitution in Eq. (54), these approximations lead to

$$F_{xx} \approx \alpha_x\ \Gamma_x\ P_\Gamma. \tag{55}$$

For $x \neq y$, χ_{xy} is a measure of the correlation between the left and right lead with M^{xy} as $N_l \times N_r$ as the left-right (lr) channel matrix. Assuming negligible correlations among matrix elements of M^{lr}, one can approximate:

$$\chi_{\mathrm{lr}}^2 \approx \sum_{p,q}\left(M_{pq}^{\mathrm{lr}}\right)^2\gamma_{pl}^2\ \gamma_{qr}^2 \approx \alpha_c^2\sum_{p,q}\gamma_{pl}^2\ \gamma_{qr}^2, \tag{56}$$

with

$$\alpha_c = \left\langle M_{pq}^{\mathrm{lr}}\right\rangle_{p,q} \tag{57}$$

is the average matrix element of the left-right (lr) channel matrix. Equation (54), then gives

$$F_{\mathrm{lr}} = F_{\mathrm{rl}} \approx \alpha_c\ (\Gamma_l\ \Gamma_r)^{1/2}\ P_\Gamma. \tag{58}$$

Substitution of J_1, J_2, J_3 along with approximations [Eqs. (55) and (58)] in Eq. (45) leads to diffusion equation for P_Γ:

$$\begin{aligned}\frac{1}{4}\frac{\partial P_\Gamma}{\partial\Lambda_\psi} = &\sum_{x=l,r}\frac{\partial}{\partial\Gamma_x}\left[\frac{\partial}{\partial\Gamma_x}[\Gamma_x(\alpha_x-\Gamma_x)P_\Gamma]\right.\\ &\left.+\frac{1}{2}(N\Gamma_x - N_x\ \alpha_x)P_\Gamma\right]\\ &+2\frac{\partial^2}{\partial\Gamma_l\partial\Gamma_r}[\alpha_c\sqrt{\Gamma_l\Gamma_r} - \Gamma_l\Gamma_r]P_\Gamma.\end{aligned} \tag{59}$$

Equation (59) describes the diffusion of the joint distribution of the left and right resonance widths due to varying dot conditions. It can now be used to derive the diffusion equation for the peak-height distribution.

C. Diffusion equations for the peak heights

Following Eq. (4), the distribution $P(g)$ of the conductance-peak height $g = (\overline{\Gamma}/2)\ g_\psi$ for a single resonance level Ψ can be expressed as

$$P_g(g) = \int \delta\left(g - \frac{\Gamma_l\Gamma_r}{\Gamma_l+\Gamma_r}\right)P_\Gamma\ d\Gamma_l\ d\Gamma_r. \tag{60}$$

This gives

$$\frac{\partial P_g}{\partial\Lambda_g} = \int \delta\left(g - \frac{\Gamma_l\Gamma_r}{\Gamma_l+\Gamma_r}\right)\frac{\partial P_\Gamma}{\partial\Lambda_\psi}\ d\Gamma_l\ d\Gamma_r, \tag{61}$$

where $\Lambda_g = 4\Lambda_\psi$.

Using Eq. (59) and integrating partially as in the previous cases, we get

$$\begin{aligned}\frac{\partial P_g}{\partial\Lambda_g} = &\frac{\partial^2}{\partial g^2}\{g(s-g)\ P_g + Q_2\}\\ &+\frac{1}{2}\frac{\partial}{\partial g}\{(Ng-\theta)P_g + 2Q_1\},\end{aligned} \tag{62}$$

where

$$\begin{aligned}&\theta = \tfrac{1}{2}\ (N_l\alpha_l + N_r\alpha_r), \quad \phi = \tfrac{1}{2}\ (N_l\alpha_l - N_r\alpha_r),\\ &s = \tfrac{1}{2}\ (\alpha_l+\alpha_r), \quad r = \tfrac{1}{2}\ (\alpha_l-\alpha_r),\end{aligned} \tag{63}$$

with $\alpha' s$ defined by Eqs. (53) and (57) and

$$\begin{aligned}Q_n(g) = g^{2n}&\int \delta\left(g - \frac{\Gamma_l\Gamma_r}{\Gamma_l+\Gamma_r}\right)\left(\frac{1}{\Gamma_l\Gamma_r}\right)^3\\ &\times v_n(\Gamma_l,\Gamma_r)\ P_\Gamma\ d\Gamma_l\ d\Gamma_r,\end{aligned} \tag{64}$$

with $n = 1,2$ and

$$\begin{aligned}v_1(x,y) = &(\theta+2s)x^2y^2 - xy(x+y)^{-1}\mathbf{(}2xy\Omega + 2r(y^3-x^3)\mathbf{)}\\ &-(\phi+4r)(y^2-x^2)xy/2,\\ v_2(x,y) = &xy\mathbf{(}\Omega - 3s(x+y)\mathbf{)} + r(y^3-x^3),\end{aligned} \tag{65}$$

with $\Omega = 2\alpha_c\sqrt{xy}$.

The relation $\delta(z - \frac{xy}{x+y}) = \frac{y^2}{z^2}\delta(y - \frac{zx}{x-z})$ simplifies Q_n:

$$Q_n(g) = g^{n-1}\int w_n(g,\Gamma_l)\ \frac{\Gamma_l^2}{(\Gamma_l-g)^2}\ P_\Gamma\left(\Gamma_l, \frac{g\Gamma_l}{\Gamma_l-g}\right)\ d\Gamma_l, \tag{66}$$

with

$$\begin{aligned}w_1(g,x) = &(\theta+2s)g\frac{(x-g)}{x^2} - 2g\Omega\frac{(x-g)^2}{x^4}\\ &-2r\frac{\mathbf{(}g^3-(x-g)^3\mathbf{)}}{x^3} - (\phi+4r)\frac{\mathbf{(}g^2-(x-g)^2\mathbf{)}}{2x^2},\end{aligned} \tag{67}$$

$$w_2(g,x) = \frac{(x-g)^2}{x^4}g\Omega - 3sg\frac{(x-g)}{x^2} + r\frac{\mathbf{(}g^3-(x-g)^3\mathbf{)}}{x^3}. \tag{68}$$

Equation (62) describes the Λ_g-governed diffusion of the conductance distribution for dots under generic conditions, with a nonzero correlation between left and right leads. The correlations between different channels in the lead, however, are assumed to be weaker than the self-correlation. The

presence of w_n makes it difficult to express U_n as functions of g only; it can, however, be achieved by system-specific approximations.

Linear relation between left and right resonance widths. For example, here we consider the case with $\Gamma_r \sim q\Gamma_l$. At $\Gamma_r = q\Gamma_l$, $g = \frac{q}{q+1}\Gamma_l$ with q as a system-dependent constant. Taylor series expansion of $w_n(g,\Gamma_l)$ in the neighborhood of $\Gamma_l = \eta g$ with $\eta = (q+1)/q$ leads to $w_n(g,\Gamma_l) = w_n(g,\eta g) + \sum_{k=1}^{\infty} \frac{\partial^k w_n(g,\Gamma_l)}{\partial \Gamma_l^k}(\Gamma_l - \eta g)^k$. For the case $\Gamma_r \sim q\Gamma_l$, the dominant contribution comes from the first term, which results in

$$Q_n(g) \approx g^{n-1}\ w_n(g,\eta g)\ P(g), \tag{69}$$

where the relation $P_g(g) = \int \frac{\Gamma_l^2}{(\Gamma_l - g)^2}\ P_\Gamma(\Gamma_l, \frac{g\Gamma_l}{\Gamma_l - g})\ d\Gamma_l$ is used. Equation (62) can now be rewritten as

$$\frac{\partial P_g}{\partial \Lambda_g} = \frac{\partial^2}{\partial g^2}[g\ (t_2 - g)]P_g + \frac{1}{2}\frac{\partial}{\partial g}[Ng - t_1]P_g, \tag{70}$$

where

$$t_1 = \theta - 2(\theta + 2s)\frac{(\eta-1)}{\eta^2} + 8\alpha_c\frac{(\eta-1)^{3/2}}{\eta^3} + 4r\frac{\mathbf{(}1-(\eta-1)^3\mathbf{)}}{\eta^3} + 2(\phi/2 + 2r)\frac{(2-\eta)}{\eta}, \tag{71}$$

$$t_2 = 2\alpha_c\frac{(\eta-1)^{3/2}}{\eta^3} + s\left(1 - 3\frac{(\eta-1)}{\eta^2}\right) + r\frac{\mathbf{(}1-(\eta-1)^3\mathbf{)}}{\eta^3},$$

where θ,ϕ,s,r are given by Eq. (63). Equation (70) describes the diffusion of peak-height distribution of a Coulomb blockade dot under varying conditions. Here Λ_g contains the information about dot conditions (e.g., shape, disorder, and interaction strength) while t_1, t_2 depend only on the lead details. Our next step is to solve Eq. (70) to obtain the peak-height distribution.

V. PEAK-HEIGHT DISTRIBUTION: SOLUTION OF EQ. (70)

Changing the variable $g \to t_2\ z$, followed by a substitution of $P_z(z,\Lambda_g) = \Upsilon(z)e^{-E\Lambda_g}$ and a rearrangement of terms, reduces Eq. (70) in the well-known form of a hypergeometric differential equation:

$$z(1-z)\frac{d^2\Upsilon}{dz^2} + \{c - (1+a+b)z\}\frac{d\Upsilon}{dz} - ab\Upsilon = 0, \tag{72}$$

where

$$a = \frac{1}{4}[6 - N + \sqrt{(N-2)^2 + 16E}], \tag{73}$$

$$b = \frac{1}{4}[6 - N - \sqrt{(N-2)^2 + 16E}], \tag{74}$$

$$c = 2 - \frac{t_1}{2t_2}. \tag{75}$$

The general solution of Eq. (72) depends on whether c is an integer or not. As Eq. (75) along with Eq. (71) implies, c is in general a fraction. Thus we have for $|z| < 1$,

$$\Upsilon(z) = AF(a,b;c;z) + Bz^{1-c}F \times (1+a-c, 1+b-c; 2-c; z), \tag{76}$$

with A,B as arbitrary constants and the hypergeometric function $F(a,b;c;z)$ defined as

$$F(a,b,c;z) \equiv {}_2F_1(a,b;c;z) = 1 + \sum_{k=1}^{\infty}\frac{(a)_k\ (b)_k}{(c)_k}\frac{z^k}{k!}, \tag{77}$$

with $(q)_k = q(q+1)\ldots(q+k-1)$. The arbitrary constants A,B can easily be determined if F can be expressed as an orthogonal polynomial. This can be achieved, without loss of generality, by taking $b = -n$ which gives $a = n + 3 - \frac{N}{2}$ and $E = \frac{1}{2}(n+1)(2n+4-N)$.

The finiteness of $P(z,\Lambda_g)$ for large Λ_g requires $E = \frac{1}{2}(1-b)(4-N-2b) \geqslant 0$ or $b \leqslant 2 - N/2$. Taking $b = 2 - m - N/2$ gives $a = m + 1$ [see Eqs. (73) and (74)]. The general form of $P(z,\Lambda_g)$ then becomes

$$P(z,\Lambda_g) = \sum_{m=0}^{\infty} \mathrm{e}^{-\frac{1}{2}(N+2m-2)m\Lambda_g}\ \Upsilon_m(z), \tag{78}$$

where

$$\Upsilon_m(z) = A_m\ f_1(m,z) + B_m\ z^{1-c}\ f_2(m,z), \tag{79}$$

with

$$f_1 = F(m+1, 2-m-N/2; c, z), \tag{80}$$

$$f_2 = F(m+2-c, 3-m-N/2-c; 2-c; z). \tag{81}$$

Using the identity,

$$F(a,b;c;z) = (1-x)^{c-a-b}F(c-a, c-b; c; z), \tag{82}$$

f_1 and f_2 can be rewritten as

$$f_1(m,z) = (1-z)^{c-3+N/2} \times F(c-m-1, c-2+m+N/2; c; z) \tag{83}$$

$$\approx (1-z)^{c-3+N/2}\Phi(c-m-1; c, Nz/2), \tag{84}$$

$$f_2(m,z) = (1-z)^{c-3+N/2}F\mathbf{(}-m, (N/2+m-1); 2-c, z\mathbf{)} \tag{85}$$

$$\approx (1-z)^{c-3+N/2}\Phi(-m, 2-c; Nz/2) \tag{86}$$

$$= \frac{\Gamma(m+1)\Gamma(2-c)}{\Gamma(m+2-c)}\ \mathrm{e}^{-(c-3+N/2)z}\ L_m^{1-c}(Nz/2), \tag{87}$$

where Eqs. (84) and (87) follow under large N approximation and $L_m^a(z)$ refers to the associated Laguerre polynomial of m^{th} order.

For large N and c noninteger, f_1 diverges for $z \geqslant 1$. The finiteness of $P(z,\Lambda)$ therefore requires $A_m = 0$. The initial condition $P(z,0)$ along with orthogonality of Laguerre polynomials gives B_m as follows:

$$B_m = \left(\frac{N}{2}\right)^{2-c}\ \frac{1}{\Gamma(2-c)}\ \int L_m^{1-c}(Nz/2)\ P(z,0)\ dz. \tag{88}$$

With substitution of A_m, B_m in Eq. (79), followed by the transformations $g = t_2 z$ and $P(g) = (1/t_2)P(z)$, Eq. (78) leads to

$$P(g,\Lambda_g) = t_2^{-1}\sum_{m=0}^{\infty} B_m\ d_m\ e^{-\frac{1}{2}(N+2m-2)m\Lambda_g} \times e^{-Ng/2t_2}\ (g/t_2)^{1-c}\ L_m^{1-c}(Ng/2t_2), \tag{89}$$

where $d_m = \frac{\Gamma(m+1)\Gamma(2-c)}{\Gamma(m+2-c)}$.

Equation (89) describes the conditional peak-height distribution $P(g,\Lambda)$ of a dot for an arbitrary initial condition $P(g,0)$ and under generic system conditions. In the limit $\Lambda \to \infty$ [which corresponds to the Wigner-Dyson limit of the dot Hamiltonian, see the discussion below Eq. (11)], the distribution evolves to (as only the $m = 0$ term contributing)

$$P(g,\infty) = \frac{N}{2\,\Gamma(2-c)\,t_2}\left(\frac{N\,g}{2\,t_2}\right)^{1-c} \mathrm{e}^{-\frac{N\,g}{2\,t_2}}. \qquad (90)$$

The presence of lead parameters c and t_2 in Eq. (90) indicates that, even for chaotic dots with weak disorder (the regime where the dot Hamiltonian is well modeled by a Wigner-Dyson ensemble), the peak-height statistics is sensitive to the dot-lead interactions.

The solution for a finite Λ_g depends on the choice of $P(g,0)$. A suitable initial condition is $P(g,0) = \delta(g)$ which corresponds to the quantum dot in an insulator regime. For this condition, Eq. (88) gives $B_m = (\frac{N}{2})^{2-c}\,\frac{1}{d_m\Gamma(2-c)}$. Using the relation $\Gamma(m+1)\,L_m^a(z) = z^{-a/2}e^z \int y^{m+a/2}\,e^{-y}\,J_a(2\sqrt{zy})\,dy$ in Eq. (89), we get

$$P(g,\Lambda_g) = \frac{N}{2\,\Gamma(2-c)\,t_2}\left(\frac{Ng}{2\,t_2}\right)^{\frac{(1-c)}{2}} \times \int_0^\infty y^{\frac{(1-c)}{2}} e^{-y\tau} J_{1-c}\left(\sqrt{\frac{2Ngy}{t_2}}\right) dy \qquad (91)$$

$$= \frac{N}{2\,\Gamma(2-c)\,t_2\tau}\left(\frac{Ng}{2\,t_2\tau}\right)^{1-c} e^{-Ng/2t_2\tau} \quad (\text{for } c<2), \qquad (92)$$

with $\tau = 1 - \mathrm{e}^{-N\Lambda_g/2}$ as a function of dot parameters c,t_2 as lead parameters.

For $c > 2$, $P(g,\Lambda_g)$ can be expressed in the form of a series,

$$P(g,\Lambda_g) = \frac{N}{2\,\Gamma(2-c)\,t_2\tau}\left(\frac{2Ng}{t_2}\right)^{\frac{(1-c)}{2}} \times \sum_{k=0}^{\infty} \frac{(-1)^k}{\Gamma(2-c+k)}\left(\frac{Ng}{t_2\tau}\right)^k. \qquad (93)$$

Equations (89), (92), and (93) indicate that the dot information affects the conductance distribution only through a single parameter, namely, $\tau/2N$. The lead information also enters in the formulation only through two parameters (i.e., t_1,t_2). The dot-lead systems with different conditions may correspond to the same Λ,t_1,t_2 and thus same peak-height statistics. Note the distribution has a weak dependence on Λ_g and therefore on the dot conditions; this can be visualized from Fig. 1 which depicts the behavior of $P(\ln g)$ for a given pair of leads but for varying dot conditions (measured by $b = \tau/2N$). Figure 2 depicts the measure for the same dot but for a different pair of leads. The suggested weak sensitivity to dot conditions in our formulation is in agreement with numerically observed almost similar peak-height fluctuations for ballistic dots with various shape deformations.[22] The appearance of the term g^{1-c} in Eqs. (89) (92), and (93), however, suggests a strong influence on the lead conditions. This can be visualized from Fig. 3, depicting $P_g(\ln g)$ for a given dot attached to different leads.

The influence of the dot-lead conditions can be more clearly seen by a rescaling of g in Eq. (92) by $2t_2\tau/N$. This leads to a

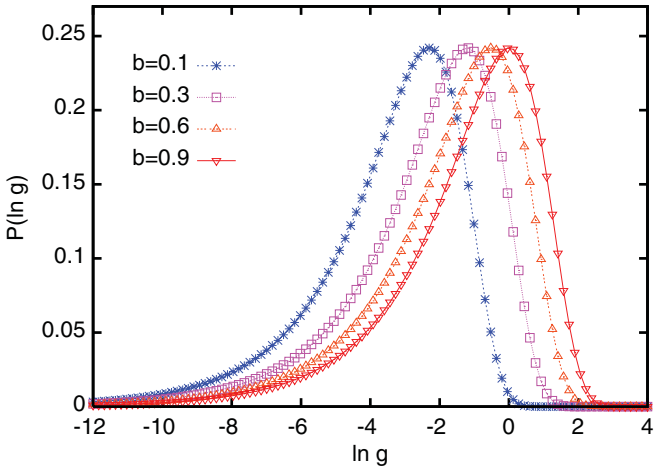

FIG. 1. (Color online) Distribution $P(\ln g)$ [Eq. (92)] for a given pair of leads at different dot parameters $b = (1 - \mathrm{e}^{-N\Lambda})/2N$. The lead parameters are fixed at $c = 1.5$, $t_2 = 0.5$.

form, independent of the dot conditions and a single parametric dependence on the leads:

$$P(g_s,\Lambda_g) = \frac{1}{\Gamma(2-c)}\; g_s^{1-c}\; e^{-g_s}, \qquad (94)$$

with $g_s = Ng/2t_2\tau = N\overline{\Gamma}g_\Psi/4t_2\tau$. Note the removal of N dependence by a rescaling of g indicates an *almost* independence of the peak-height statistics from the number of interacting electrons. This is in accordance with the experimental observations.[1]

As examples, we consider two limiting cases of the lead conditions:

(i) *Almost symmetric dots*. In this case, left and right resonance widths are almost equal (i.e., $\Gamma_l = \Gamma_r$), which gives $\eta = 2$. Further assuming $\alpha_l = \alpha_r = \alpha_c$ and $N_l = N_r \equiv N_c$, which implies $r = 0$, $\theta = sN_c$, $\phi = 0$ [see Eq. (63)], we get from Eq. (71),

$$t_1 = \frac{sN_c}{2}, \quad t_2 = \frac{s}{2}, \qquad (95)$$

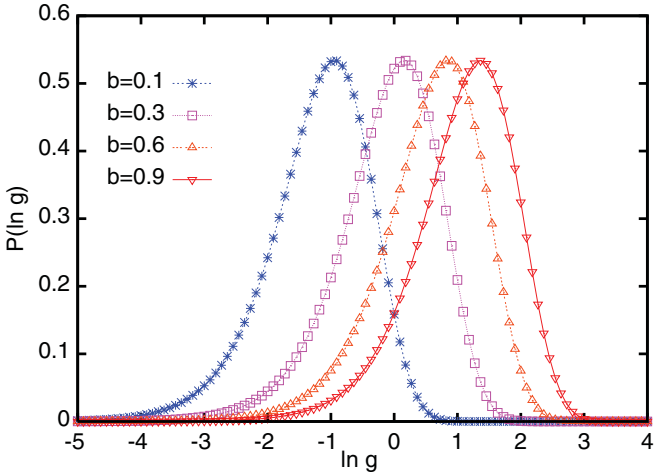

FIG. 2. (Color online) As in Fig. 1 but with a different pair of leads with lead parameter fixed at $c = 0.05$, $t_2 = 0.5$.

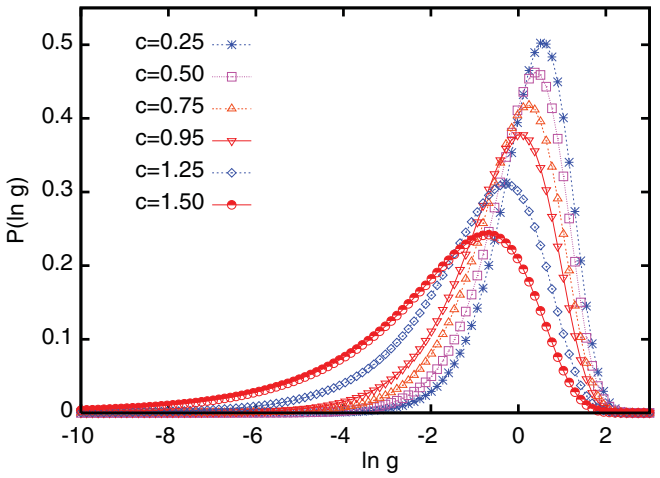

FIG. 3. (Color online) Distribution $P(\ln g_s)$ [Eq. (94)] for a given dot under different lead conditions (different c).

and, therefore, from Eq. (75), $c = 2 - N_c/2$. For almost symmetric chaotic dots (i.e., $\Lambda \to \infty$), Eq. (92) then gives a χ^2 distribution in N_c degrees of freedom:

$$P(g,\infty) \propto g^{(\frac{N_c}{2}-1)}\, e^{-Ng/2s}. \tag{96}$$

The result is in agreement with Eq. (31) of Ref. 17 for the case of chaotic dots attached to symmetric leads with equivalent and uncorrelated channels (Note the $\lambda = 0$ case depicted in Fig. 4 of Ref. 17 is a χ^2 distribution in Λ degrees of freedom with Λ as the number of channels in this study).

(ii) *Asymmetric dots*. Contrary to the previous case, Γ_l and Γ_r in this case are very different. Consider $q = \frac{\Gamma_r}{\Gamma_l} \ll 1$, which gives $\eta \gg 1$ and therefore from Eq. (71),

$$t_1 = \theta - \phi - 8r = (N_r + 4)\alpha_r - 4\alpha_l, \qquad t_2 = s - r = \alpha_r, \tag{97}$$

and $c = 2\frac{\alpha_l}{\alpha_r} - \frac{N_r}{2}$ [see Eq. (75)]. For asymmetric chaotic dots (i.e., $\Lambda \to \infty$), then Eq. (92) gives

$$P(g,\infty) \propto g^{(1+\frac{N_r}{2}-2\frac{\alpha_l}{\alpha_r})}\, e^{-Ng/2\alpha_r}. \tag{98}$$

For the leads with $\alpha_l \approx \alpha_r$, Eq. (98) then gives a χ^2 distribution, which is consistent with the semiclassical study of[14] on the chaotic dots with asymmetric leads [see Eq. (49) of Ref. 14]. For cases $\alpha_r \ll \alpha_l$, Eq. (98) implies a higher probability of nearly zero conductance in the asymmetric case as compared to the symmetric case.

The reverse limit of $q \gg 1$ gives $\eta = 1$, which in turn leads to $c = 2\frac{\alpha_r}{\alpha_l} - \frac{N_l}{2}$ [as in this case $t_1 = (N_l + 4)\alpha_l - 4\alpha_r$, $t_2 = \alpha_l$]. Thus, following an interchange of the subscripts $l \to r$, Eq. (98) describes the distribution in this case, too.

For comparisons with previous studies and for future applications, it is important to summarize the approximations used in our derivation:

(i) The assumption of the dominance of diagonal elements of the channels correlation matrix over off-diagonals (required to obtain the closed form diffusion equation for the partial widths from that of the partial-width amplitudes) and replacing each diagonal by the average diagonal α_x to approximate F_{xx} [see Eq. (55)];

(ii) The replacement of the left-right channel matrix element $M^{\rm lr}$ by its average α_c [see Eq. (58)];

(iii) The assumption of the linearized relation between left and right partial widths to obtain Eq. (70) from Eq. (62);

(iv) The conductance peaks due to different resonance levels are also assumed to be uncorrelated; the assumption is justified at temperatures $\overline{\Gamma} < T < \Delta$ only.

Although valid for generic dot conditions, the above approximations restrict the applicability of our results to the leads with weakly correlated channels. Note an analytical expression for $P_g(g)$ for the irregularly shaped dots with multichannel leads (for any number of nonequivalent and correlated channels) was derived in Refs. 16 and 17 (for other related studies see Refs. 18–21). This study assumes the statistical properties of the resonance eigenfunction to be that of a Wigner-Dyson ensemble and is therefore applicable only in the chaotic regime and/or weak-disordered limit. These studies correspond to the $\Lambda \to \infty$ limit of our formulation.

The approximations used in our analysis make it desirable to compare our results with numerical/experimental studies of generic QCB dots. Unfortunately almost all such previous studies focus on the peak-spacing distribution, with very few results available for the peak-heights distribution. A proper numerical verification of our results is a time-consuming process; it requires the simulations of large random-matrix ensembles of thousands of matrices for many combinations of the dot-lead conditions. We intend to report these results in the near future.

VI. CONCLUSION

Using a complexity parameter-governed diffusion equation [Eq. (9)] for the components of a resonance eigenfunction, we analytically derive the single-level conductance-peak height distribution in the QCB regime of a quantum dot under generic conditions. The essence of our formulation is the maximum entropy hypothesis, which permits the representation of the dot Hamiltonian by a multiparametric Gaussian ensemble. This is because the existing dot conditions (e.g., shape, disorder, two-body interaction strength) subject matrix elements to varying constraints; the entropy maximization under these constraints leads to their different distribution parameters. The statistical behavior of the ensemble, however, is mainly governed by the complexity parameter Λ,[12] which is essentially the mean-square off-diagonal matrix element measured in units of the square of the local mean level spacing.

The Λ formulation reveals insensitivity of the peak-height distribution to microscopic details of the dot's conditions: The distribution is the same for different dots if they share the same Λ and belong to same global constraint class (e.g., antiunitary symmetry). (A calculation of Λ requires a knowledge of some past state of dot and same global conditions for different dots allow use of a common initial condition; see Ref. 15 for details). The formulation helps one to quantify the robustness of fluctuations to varying dot conditions as well as in seeking analogous behavior in seemingly different dots.

Some studies in the past have claimed the observations of the fractal nature of peak heights.[23,24] These observations intuitively seem to be in accordance with our Λ-based formulation. The eigenfunction statistics being multifractal at

the critical value Λ_* of the complexity parameter (see Ref. 13), it is expected to influence peak-height statistics. However, our prediction that the fractal peak heights will occur at Λ_* is yet to be verified.

The peak-height distribution obtained here is applicable only for the temperature regimes $T \ll \Delta$. For $T \sim \Delta$, thermal fluctuations of the electron energy in the leads allow conductance to occur through several resonances. The experimentally observed correlations among peaks at higher temperatures require a knowledge of the joint distribution of the conductance-peak heights $P(g_1, g_2, \ldots, g_N)$ and therefore the joint distribution function of many resonance eigenfunctions. Using Eq. (25) of Ref. 13 instead of Eq. (9) and proceeding essentially in the same way as given in Sec. III, the diffusion equation for $P(g_1, g_2, \ldots, g_N)$ can be derived; the increased number of variables in this case makes the derivation messy. It would also be interesting to apply the system-dependent random-matrix approach to other energy scales (e.g., where co-tunneling exists). Another important regime is where exchange interaction plays a dominant role leading to an experimentally observed spin pairing. Although the dot's spin is experimentally reported not to significantly influence the peak-height distribution, it leaves its imprints on the peak-to-peak correlations and the peak-spacing distribution. Intuitively, the spin pairing in our model will lead to inhomogeneous interactions, and, consequently change in Λ and a different level statistics; we intend to pursue the question in the near future.

The present study deals with the dots with time-reversal symmetry. Similar information is required for the dots in a slowly varying magnetic field or the dots with/without other unitary/antiunitary symmetries. We hope to report some of these studies in the near future.

ACKNOWLEDGMENT

We thank Michael Berry for many helpful discussions and technical suggestions.

[1] Y. Alhassid, Rev. Mod. Phys. **72**, 895 (2000).
[2] M. L. Mehta, *Random Matrices*, 2nd ed. (Academic, New York, 1991).
[3] R. Jalbert, A. D. Stone, and Y. Alhassid, Phys. Rev. Lett. **68**, 3468 (1992).
[4] S. R. Patel, D. R. Stewart, C. M. Marcus, M. Gokcedag, Y. Alhassid, A. D. Stone, C. I. Duruoz, and J. S. Harris Jr., Phys. Rev. Lett. **81**, 5900 (1998).
[5] U. Sivan, R. Berkovits, Y. Aloni, O. Prus, A. Auberbach, and G. Ben-Yoseph, Phys. Rev. Lett. **77**, 1123 (1996).
[6] R. Berkovits, Phys. Rev. Lett. **81**, 2128 (1998).
[7] M. Kastner, Rev. Mod. Phys. **64**, 892 (1992).
[8] I. L. Kurland, I. L. Aleiner, and B. L. Altshuler, Phys. Rev. B **62**, 14886 (2000).
[9] P. W. Brouwer, Y. Oreg, and B. I. Halperin, Phys. Rev. B **60**, R13977 (1999).
[10] H. U. Baranger, D. Ullmo, and L. I. Glazman, Phys. Rev. B **61**, R2425 (2000).
[11] Y. Alhassid, Ph. Jacquod, and A. Wobst, Phys. Rev. B **61**, R13357 (2000).
[12] P. Shukla, Phys. Rev. E **71**, 026226 (2005).
[13] P. Shukla, Phys. Rev. E **75**, 051113 (2007).
[14] E. Narimanov, H. U. Baranger, N. R. Cerruti, and S. Tomsovic, Phys. Rev. B **64**, 235329 (2001).
[15] P. Shukla, J. Phys. Condens. Matter **17**, 1653 (2005).
[16] Y. Alhassid and C. H. Lewenkopf, Phys. Rev. Lett. **75**, 3922 (1995).
[17] Y. Alhassid, J. N. Hormuzdiar, and N. D. Whelan, Phys. Rev. B **58**, 4866 (1998).
[18] R. A. Jalabert, A. D. Stone, and Y. Alhassid, Phys. Rev. Lett. **68**, 3468 (1992).
[19] K. B. Efetov, Adv. Phys. **32**, 53 (1983).
[20] E. R. Mucciolo, V. N. Prigodin, and B. L. Altshuler, Phys. Rev. B **51**, 1714 (1995).
[21] H. A. Bruus and A. D. Stone, Phys. Rev. B **50**, 18275 (1994).
[22] R. O. Vallejos, C. H. Lewenkopf, and E. R. Mucciolo, Phys. Rev. B **60**, 13682 (1999).
[23] R. Ketzmerick, Phys. Rev. B **54**, 10841 (1996).
[24] A. S. Sachrajda, R. Ketzmerick, C. Gould, Y. Feng, P. J. Kelly, A. Delage, and Z. Wasilewski, Phys. Rev. Lett. **80**, 1948 (1998).